Investigation of the influence of heating sources on dust temperatures for use in complex molecule formation models

Jacob Promisel

ASTR 4998 – Senior Thesis

Advisor: Dr. Robin Garrod

Abstract:

In the growing field of astrochemistry, a main goal is to better understand the abundances and formation processes of atoms and molecules in outer space. A particular focus is on the formation of complex molecules which may eventually provide more information on the evolution of life in the universe. The interstellar medium (ISM) is an outer-space lab for chemistry to occur. Many computational models have been developed to simulate the chemistry that occurs in ISM clouds and provide a wealth of abundancy and formation process information. The models take as inputs several physical parameters to be able to simulate various different environments, from cold cores to star forming regions. It is very important to understand the lower limit of dust temperatures in these models, because it has a significant impact on the distribution of material between the gas and dust phases. It is also important to understand in what regimes certain heating methods dominate, especially in core collapse models in which the parameters are evolving over time. This paper explores the heating mechanisms employed to determine the dust temperature in ISM clouds. It also outlines the addition of gas-dust coupling as a heating and cooling source. The paper concludes with a discussion of the effects of this mechanism and what they mean for ISM chemistry models.

Introduction

While it may seem that the space in our galaxy, that which exists in between stars and their respective systems, is rather inactive and empty, in actuality, lots of important chemistry occurs there. This chemistry occurs in objects called interstellar medium (ISM) clouds. These clouds consist of two important phases in which chemistry can occur: gas and dust. Atoms and molecules in the gas phase interact with each other, radiation from nearby stars and cosmic rays to create and destroy different molecules. Meanwhile, atoms and molecules that exist on ISM dust particles also interact with each other, radiation and cosmic ray particles to form and destroy molecules and be absorbed or desorbed from a particle. Dust particles can have layers of ice compiled on them which form by the accretion of gas-phase atomic and molecular material. Most of the chemistry that occurs on dust grains happens on the surface layers rather than the inner layers of the mantle (Garrod & Pauly 2011).

This is important because the way gas-grain chemical kinetics models simulate chemistry on these grains is through thermal hopping. More specifically, random walk methods are used to iterate a particular molecule from absorption site to absorption site on a grain surface, or even to expel that molecule from the surface entirely. This process is highly dependent on the temperature of the grain. The higher the thermal energy, the more likely a molecule is to jump the potential energy barrier holding it inside a particular surface site. As the particle moves around, it can interact with other molecules and atoms to form new molecules. Thus, because the movement of molecules on grain surfaces is dependent on the temperature of the grain, we can determine that the amount and type of chemistry that occurs on these grains is also dependent on the dust temperature.

The need for a robust and complete determination of the dust temperature is therefore highly apparent. One important dust-phase process is the desorption of molecular hydrogen, H_2. At a dust temperature of 5 Kelvin H_2 sticks very effectively to dust grain surfaces. As the temperature of the grain rises, more and more H_2 is desorbed into the gas phase where it can initiate and contribute to chemical reactions. Molecular hydrogen is a catalyst for and involved in a huge fraction of ISM chemistry processes, so having an accurate measure of its abundance is crucial to making more precise predictions of observational data using the model.

For reference, a 2013 paper, “Simulations of Hot-Core Chemistry” by Dr. Robin Garrod and Susanna L. Widicus provides a good overview of the simulation methods in chemical

models and how the results are used in comparison with observational data (Garrod & Widicus 2013). For more specific literature, Dr. Garrod's 2013 paper, "A Three-Phase Chemical Model of Hot Cores: The Formation of Glycine" goes into more details about the workings of an actual chemical model called MAGICKAL that considers gas-phase, grain-surface, and bulk-ice chemistry in hot cores (Garrod 2013).

An important measure that we look for is the lower limit of the dust temperature in an ISM cloud. Dust temperature varies over an ISM cloud because, amongst other reasons, not as much dust-heating UV radiation reaches the inner regions of the cloud due to higher visual extinctions in those regions. We want to understand how this lower bound depends on different parameters so we can know exactly what we are working with in the various ISM cloud models we run.

In this paper, I outline a previously unused method of dust grain heating and cooling and explain how I implemented it into an existing code that generates a dust temperature profile over different values of visual extinction that would be seen in an ISM cloud. This new dust-heating process is dust-gas collisional heating and it results from the exchange of kinetic energy between dust and gas particles in the ISM. It is dependent on many parameters including dust grain size, gas temperature and gas density. This heating process is important because it can signify where in an ISM cloud we can expect to see strong dust-gas coupling (i.e. at high densities, high gas temps). It is especially significant in core-collapse models where densities are changing rapidly and temperature fluctuations could be large at certain points of the collapse.

I begin with an introduction to the dust-heating and dust-cooling processes already present in the code to provide an understanding of where this new process will fit in. I will then explain the science behind the gas-dust coupling process and proceed to show how it was implemented into the code with the existing methods. Then, I will show an overview of the results of this updated code. Lastly, I will provide an analysis of the new results and explain how it can affect the ISM cloud models going forward.

Existing Dust-Heating and Dust-Cooling Processes

The code began with a treatment of the heating and cooling effects of radiation on dust grains, outlined in Krügel (2008) and employed in the dust temperature model by Garrod and Pauly (2011). Radiation originates from stars surrounding ISM clouds. A particular set of stars

creates a specific field of radiation that then passes into the ISM cloud. Figure 1 shows a graphical representation of the radiation field used in our dust temperature calculations. The plot shows the radiation field parametrized by Zucconi et al. (2001) which we use with 7500 Kelvin, 4000 K, and 3000 K modified blackbodies as sources. It also factors in the cosmic microwave background (CMB) radiation.

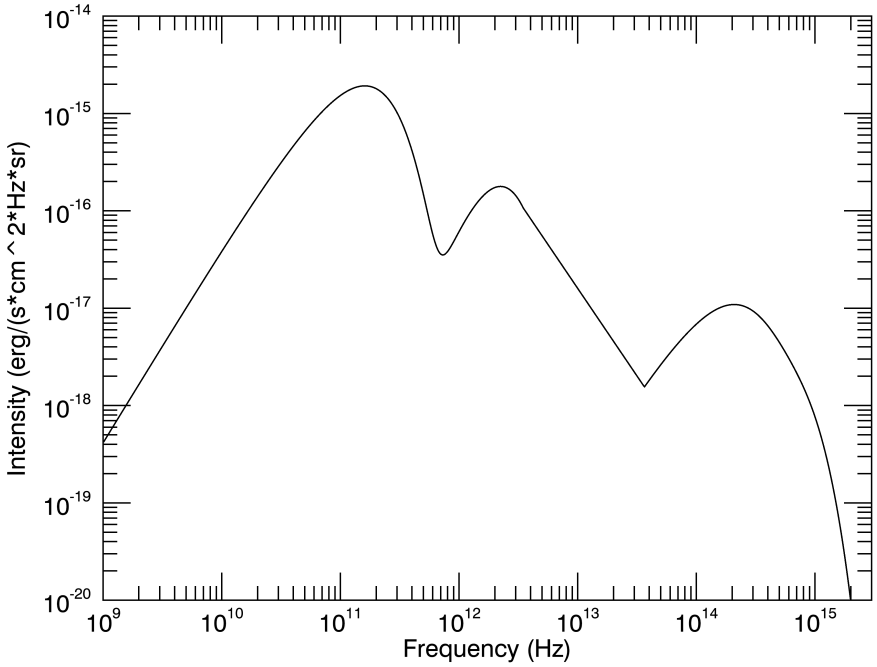

Figure 1 - Radiation field used in dust radiation heating process parametrized by Zucconi et al. (2001).

The most important type of radiation for dust-grain heating is in the ultraviolet (UV) band (from about 10^{14} - 10^{16} Hz). Note the peak in intensity in this range in our radiation field in Figure 1. The dust temperature model takes this radiation field as a heating input for dust grains and balances it with the cooling of the grain as it emits off its own thermal radiation, as per equation (1) from Krügel (2008).

$$\int Q_\nu^{abs}(a) J_\nu D_\nu(A_\nu) d\nu = \int Q_\nu^{abs}(a) B_\nu(T_d) d\nu \quad (1)$$

In equation (1), we set the left-hand side, the radiative heating effect, equal to the right-hand side, the radiative cooling effect. The Q value is an efficiency term that tells at what percentage the radiation is either absorbed or emitted by the dust grain. This efficiency term is dependent on both the grain size and the frequency of radiation. We are assuming that the absorption and emission coefficients are equal. The J term is the radiation field intensity at a

particular frequency, and the B term is a Planck function for the particular dust temperature. The D term takes a value of a visual extinction, A, and calculates the attenuation of the radiation intensity at that extinction. The code uses the radiation field intensities in Figure 1 and integrates over all frequencies to solve for the dust temperature term, T_d, at all visual extinctions.

This radiative balancing process accounts for the majority of the dust heating. Another process that can add to the heating of dust grains is the cosmic ray UV radiation field. The field arises from cosmic ray particles interacting with H_2 molecules which then emit UV photons as their excited electrons jump back down energy levels. Before I implemented the gas-dust coupling, I added in this cosmic ray heating source. We make the assumption that the UV radiation intensity from cosmic rays is about 10^{-4} x the intensity of the interstellar radiation field (ISRF). From Krügel (2008), we have:

$$\int J_\nu^{ISRF}\, d\nu = 3.183\times10^{-3} \text{ ergs s}^{-1} \text{ cm}^{-2} \tag{2}$$

This cosmic ray induced radiation field value was then simply added into the radiation intensity heating component. The dust temperature profiles using radiative heating and cooling as well as using both radiative and cosmic ray heating processes are shown in Figure 2. Note the

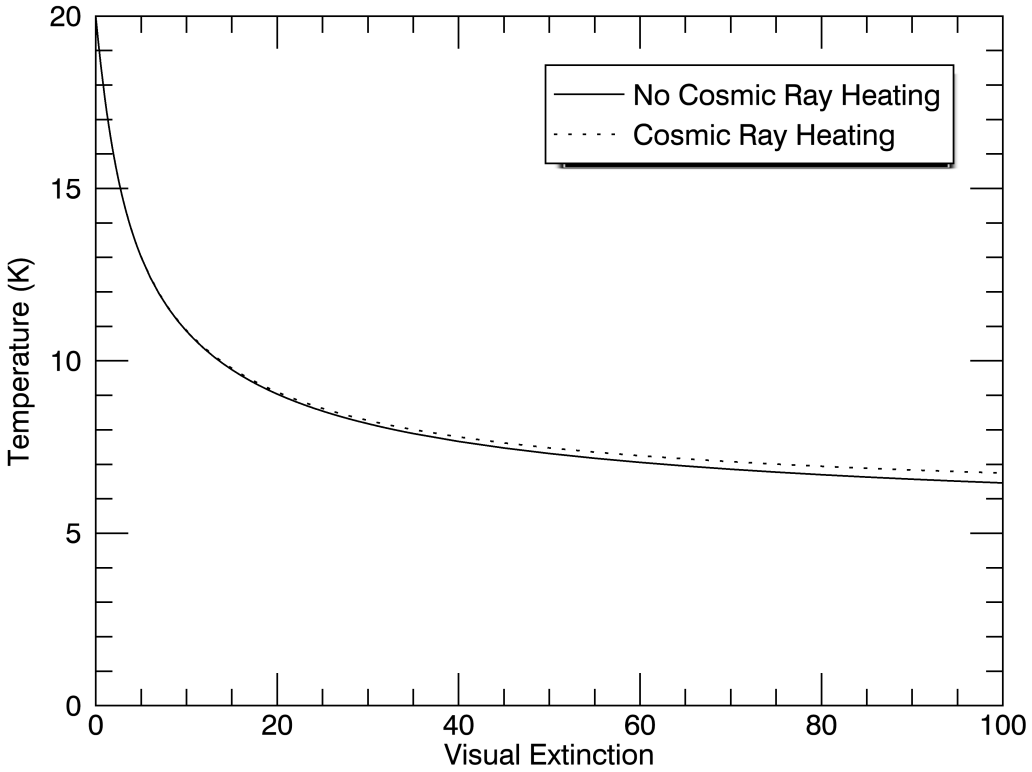

Figure 2 - Dust temperature vs. visual extinction with and without cosmic ray heating for a 0.1 micron dust grain

tail of the profiles, at high visual extinctions, has the dust temperatures at quite low values. As previously stated, the lower bound of the grain temperature is an important metric for our models. The cosmic ray heating brings this lower bound up slightly, but not to a significant degree. It may seem interesting that the cosmic ray heating has a larger effect at higher visual extinctions, but this is simply explained by the fact that the cosmic ray field does not attenuate. Cosmic ray particles can penetrate all the way through ISM clouds and so do not die in intensity like normal radiation. Thus, the induced UV field has the same intensity at all points in the cloud, while the radiation field dies and its relative strength weakens as visual extinction increases.

Figure 3 shows temperature profiles for grains of different sizes, ranging in radius from one thousandth of a micron to one micron. The relationship between grain size and temperature

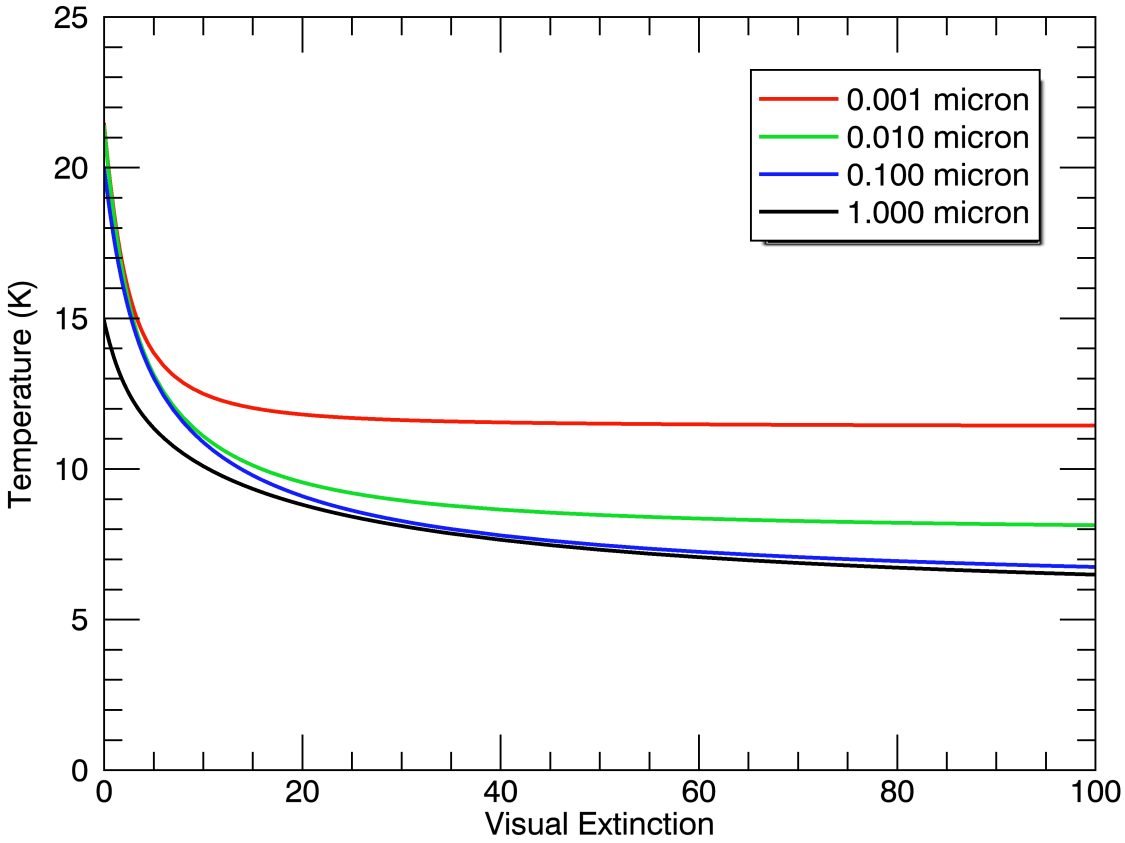

Figure 3 - Dust temperature profiles for grains of varying radii with only radiative and cosmic ray heating

is clear, larger grains remain cooler than smaller grains under the same parameters. These results make sense, as the amount of radiation absorbed scales with the cross section of the grain and the heat dissipates over the volume of the grain. Since the volume goes as the third power and the

cross section as the second, the heat dissipation term wins out and larger grains dissipate the heat more and end up colder.

Addition of Dust-Gas Coupling Mechanism

In its current state, the dust temperature model handles heating from external sources and cooling from grain emission. However, it does not consider heating and cooling from the interaction between gas and dust particles within the ISM cloud. In principal, this mechanism is quite simple: when a gas particle and a dust grain collide, they exchange kinetic energy according to equation (3) from Draine (2011).

$$\left(\frac{dE}{dt}\right)_{gas} = \sum_i n_i \left(\frac{8kT_g}{\pi m_i}\right)^{1/2} \pi a^2 \times \alpha_i \times 2k(T_g - T_d) \tag{3}$$

Here, the sum is over all of the different gas species. For our purposes, we will only consider molecular Hydrogen gas. The square root term represents the mean speed of the gas particles. The a^2 term represents the cross section of the grain, as a is the dust grain radius. This term is divided out before it's entered in the model to keep consistent with the energy per area units of the previous mechanisms. The α term is the accommodation coefficient and is a measure of inelasticity of the collisions, which we set to 1.0 for our model. The final term is the difference in kinetic energies of the dust and gas particles to determine the sign and magnitude of the energy transfer in the collision.

Equation (1) represents the old models balancing of heating and cooling sources. The collisional mechanism, as represented in Equation (3), is also a heating and cooling source, and so we can simply add it in and create a balancing equation which we then solve iteratively to get the dust temperature.

An important parameter for equation (3) is the gas density, which we are using molecular Hydrogen density for. Initial attempts at inserting this mechanism into the model used the gas density as an input parameter chosen for each run. However, there is a relationship between the visual extinction and gas density, which is shown in equation (4). This equation represents a

$$n = n(0)\left(\frac{A_v}{A_v(0)}\right)^{3/2} \tag{4}$$

valid relation between visual extinction and gas density, though it is just a choice we employed

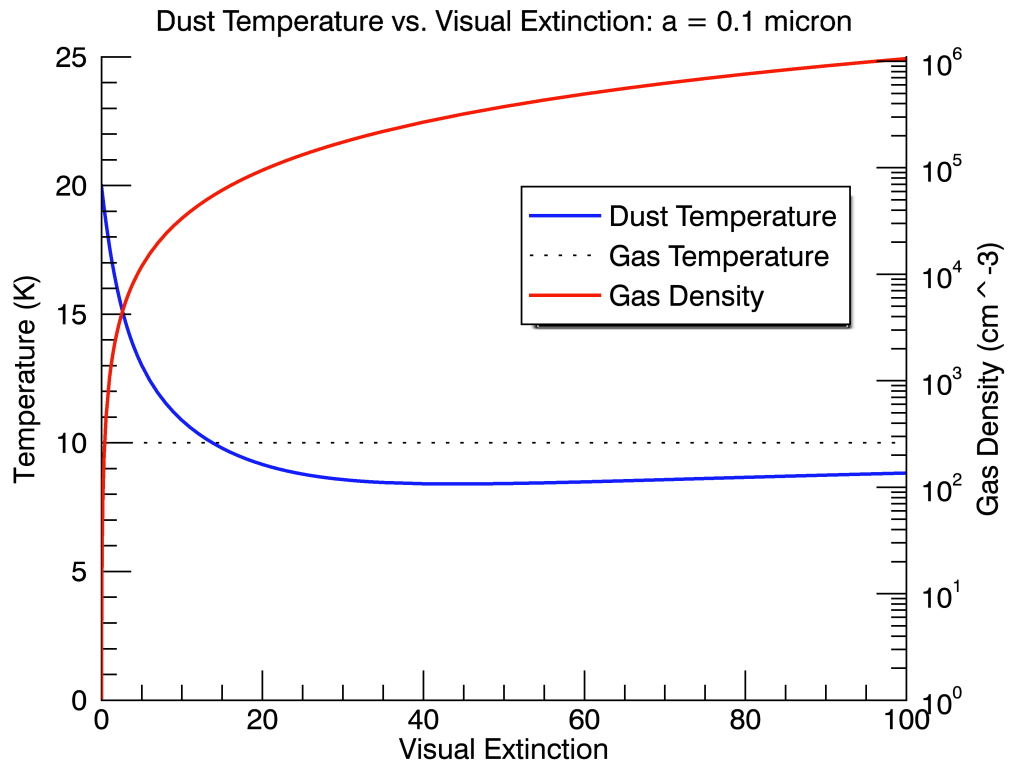

Figure 4 - temperature profile for a 0.1 micron grain and gas temperature of 10 K, with density values over visual extinction

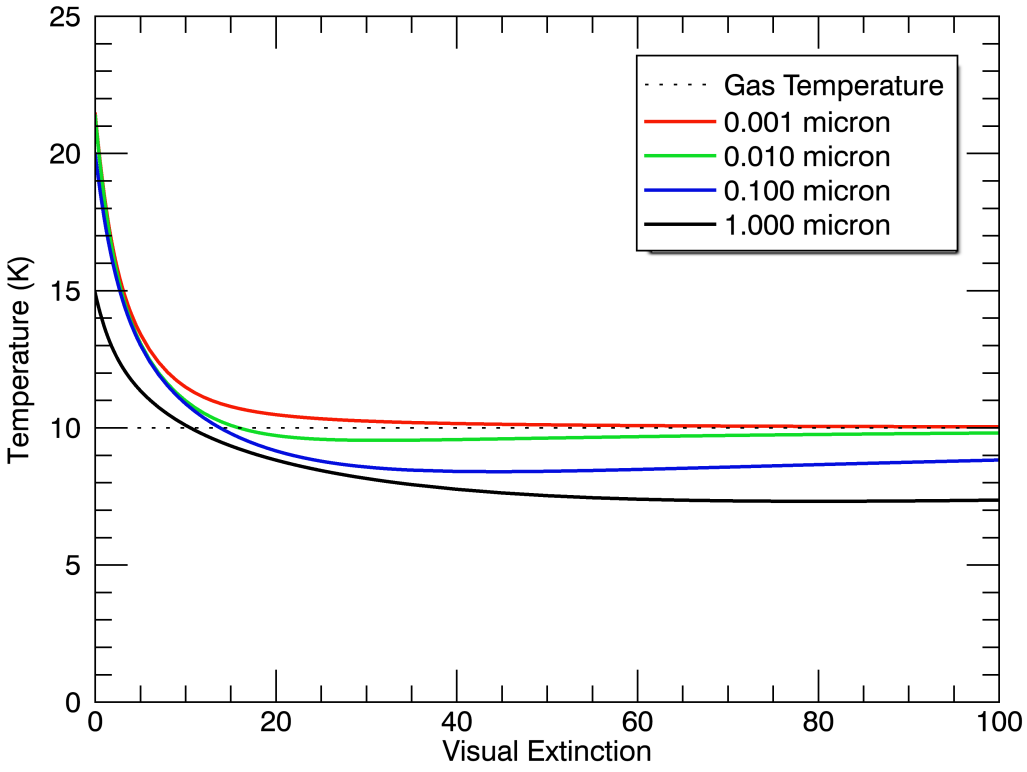

Figure 5 - temperature profiles for varying grain sizes with collisional mechanism included

for this model. The code can also be run at constant gas densities to show how dust temperatures differ with larger or higher densities at certain visual extinctions. This is especially useful because most chemistry models have a diverse range of input parameters. For reference, the appendix contains lookup values for the dust temperature and visual extinction relationship run at different densities.

We assume an initial visual extinction of 2.0 and an initial density of 3.0×10^3 cm^{-3}. As expected, the density will increase with increasing visual extinction and at an exponential rate. This is important because it means at high visual extinctions the coupling will be the dominant mechanism in most ISM models because the density will be very large, radiation will be highly attenuated, and cosmic ray heating is only a small contributor. Thus, the gas-dust coupling will be an important factor in determining the lower bound for the dust temperature in ISM clouds. We can also use the data to understand in what regimes the coupling will dominate, which can help in core collapse models when the density is constantly changing.

Figure 4 shows a dust profile with the coupling mechanism used in the model for a dust grain size of 0.1 micron. This grain radius is a good basis for our analysis as it is the standard size used in many of the chemistry simulations. Figure 4 also shows the profile of the density over the different visual extinction values, on a logarithmic scale. For this calculation we set the gas temperature to 10 Kelvin, as this is around the temperature we expect for the regions where we find our lower temperature dust grains.

Figure 5 shows the profiles for a range of grain radii from 0.001 – 1.0 micron. These runs are generated with the same density profile and gas temperature of 10 Kelvin. In the following section, I will analyze these results and compare them with the previous profiles obtained without the collisional mechanism. Then I will relate what the results tell us about dust temperatures, chemistry in ISM clouds, and other important phenomena.

Discussion

With these results, we find that the dust-gas coupling has a significant effect on the temperature profiles of interstellar dust grains. As you can see from comparing the profiles in Figure 2 and Figure 4, the tail end of the coupling profile (visual extinctions above about 20) does not fall as steeply as the non-coupling profiles. In fact, it does not fall off at all and actually rises towards the gas temperature slightly. In the radiation and cosmic ray only model, the field

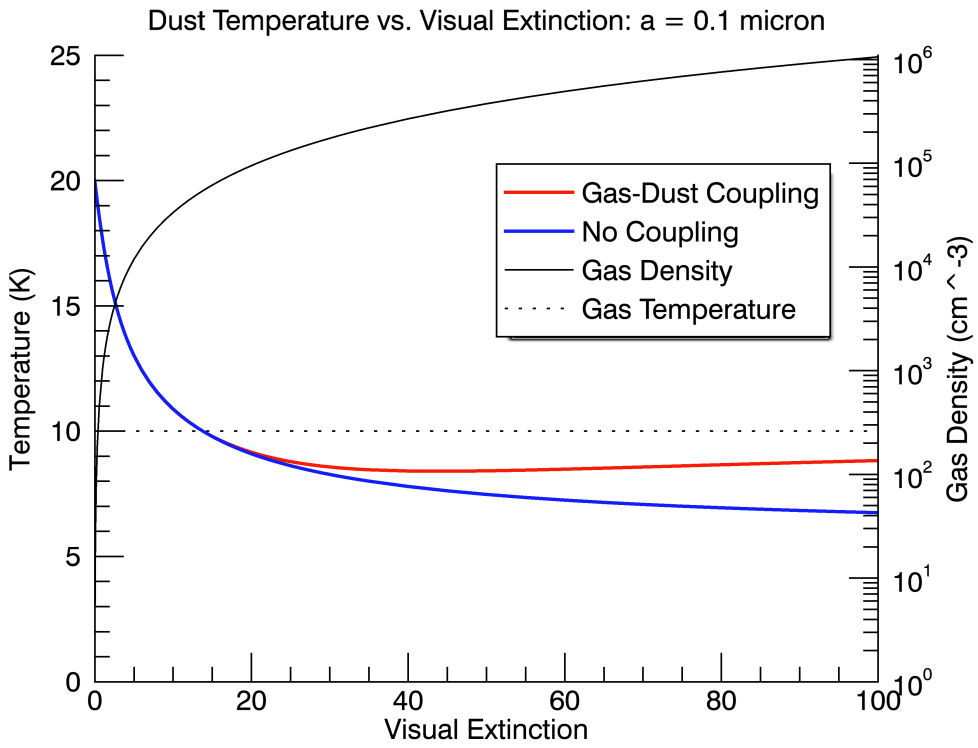

Figure 6 - Dust temperature and gas density profiles for the new (with coupling) and old (no coupling) models run at a = 0.1 micron and gas temp = 10 K

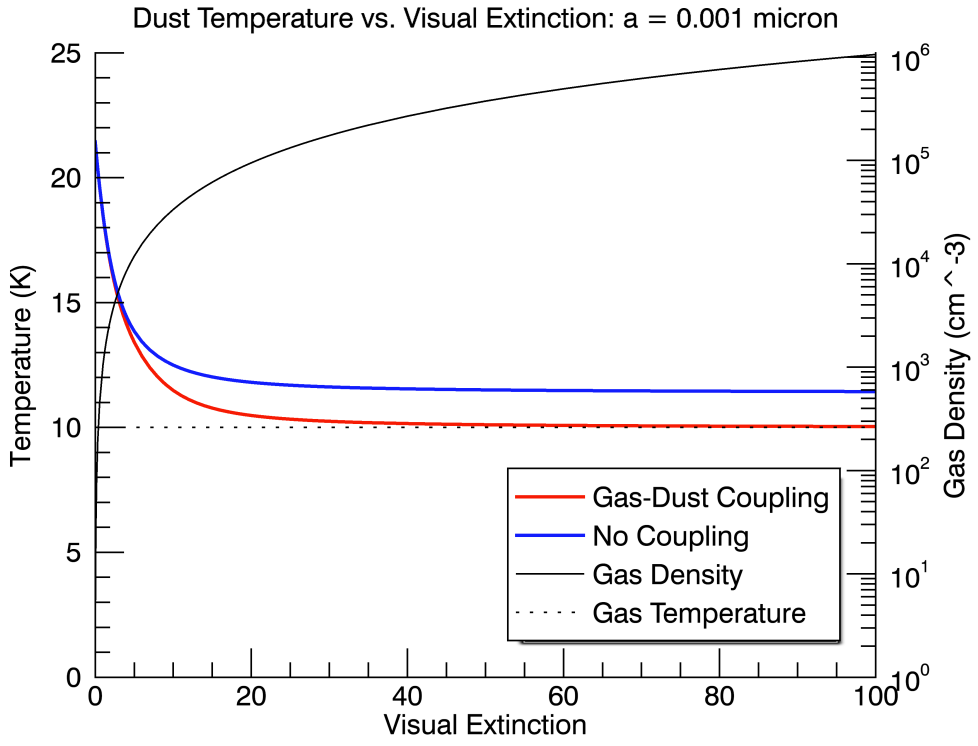

Figure 7 - Dust temperature and gas density profiles for the new (with coupling) and old (no coupling) models run at a = 0.001 micron and gas temperature = 10 K

intensity gets attenuated at high visual extinctions, and the cosmic ray contribution is small, so the effect of the heating dies out. However, in the new model, while these points stand true, the coupling actually grows in strength because the density is increasing, which can easily be seen from Equation (3). The collisional rates increase and more energy is exchanged between dust and gas particles. This can be seen in Figure 4 and Figure 5 in the profiles' tails actually converging towards the gas temperature.

Comparing the profile variations over grain sizes, both the old and new models show a trend of smaller grains having higher temperatures. However, the new model shows strong convergence to the gas temperature value at smaller grain sizes, whereas the old model reaches temperatures well above that point. This is a significant result, because it tells us that the lower bound of the dust temperature in high density, high extinction regimes where coupling can dominate is largely determined by the gas temperature.

Figure 6 gives a side by side comparison of the old and new models. Here you can easily see the differences between the two. They begin to diverge at a visual extinction of about 20 and a gas density just below 1.0×10^4 cm^{-3}. The new model profile raises the dust temperature up towards the gas temperature as collisions exchange energy between the dust and the warmer gas. Figure 7 shows the same plot run at a grain size of 0.001 micron, on the lower extreme of grains we would expect to see. It gives a good idea of how the collisional energy exchange works. For these grains, the collisional mechanism actually cools them down towards the gas temperature as the hotter grains exchange energy with the cooler gas. The profiles also begin to diverge at much lower densities (about 10^4 cm^{-3}) and visual extinctions (between 5-10).

We can see, then, that the effects of the collisional mechanism are largely infuenced by the grain size. Figure 8 gives a larger overview of the difference between the new and old models over a range of possible grain radii. Note that only for the smallest grain size did the collisional mechanism actually bring down the temperature relative to the old model, with the exception of the 0.01 micron grain between visual extinctions of about 0-15. For the profiles where the new model increased the temperature, there doesn't seem to be a clear trend over grain size. The 0.1 micron, which is the standard grain size, shows the largest differences at high visual extinctions, but smaller differences than the 0.01 micron grain at more moderate extinctions. However, while Figure 8 provides a nice visual of the effects of the new model, it is important to understand that it is very dependent on the parameters of the model. This run was done at a gas temperature of 10

Kelvin, and as we have learned, the collisional mechanism is highly coupled to the gas temperature, especially at higher extinctions and densities.

Figure 9 is the same plot run at a gas temperature of 15 Kelvin. The results are significantly different from the 10 Kelvin run. First, the new model now almost exclusively brings up the temperature (with the exception of a small blip in the 0.001 micron grain, which was negative in the 10 Kelvin run). This matches with expectations because, as stated, the collisional mechanism is strongly coupled to the gas temperature, and we have increased the gas temperature by a factor of 1.5. Second, the magnitudes of the differences are larger than the 10 Kelvin run by factors of between 2-3. Again, this matches expectations because we have raised the gas temperature well above the lower dust temperature limit seen in the old model, thus further increasing the effectiveness of the collisional heating. It can also be seen in Equation (3), which shows that the change in energy is dependent on the square root of the gas temperature and also the difference between the gas and dust temperature.

Conclusions

This new model helps us learn a few important aspects of dust grain temperatures in ISM clouds. First, we acknowledge that the addition of the collisional heating/cooling mechanism creates a significant effect, even at reasonable dust grain size and gas temperature values. It should be noted that these differences in temperature are seen mostly at higher visual extinctions and gas densities, but occur well within the range of reasonable values for these parameters in ISM clouds.

Second, we find that the gas temperature is a good proxy for the dust temperature at larger densities and visual extinctions. It is important to know that at what values this relationship will occur is strongly dependent on the size of the dust grain, all else held constant. We can, however, provide data to reference in what regimes we may expect this strong coupling dependence to occur for different grain sizes. This is very helpful in dynamic ISM models where density and extinction values vary, particularly in core collapse models in which they trend towards very large values and the coupling dependence is expected to be very strong. More accurate dust temperature readings will allow for more robust chemistry simulation in ISM models. The dust temperature adjustments will affect the movement of molecules on the grain

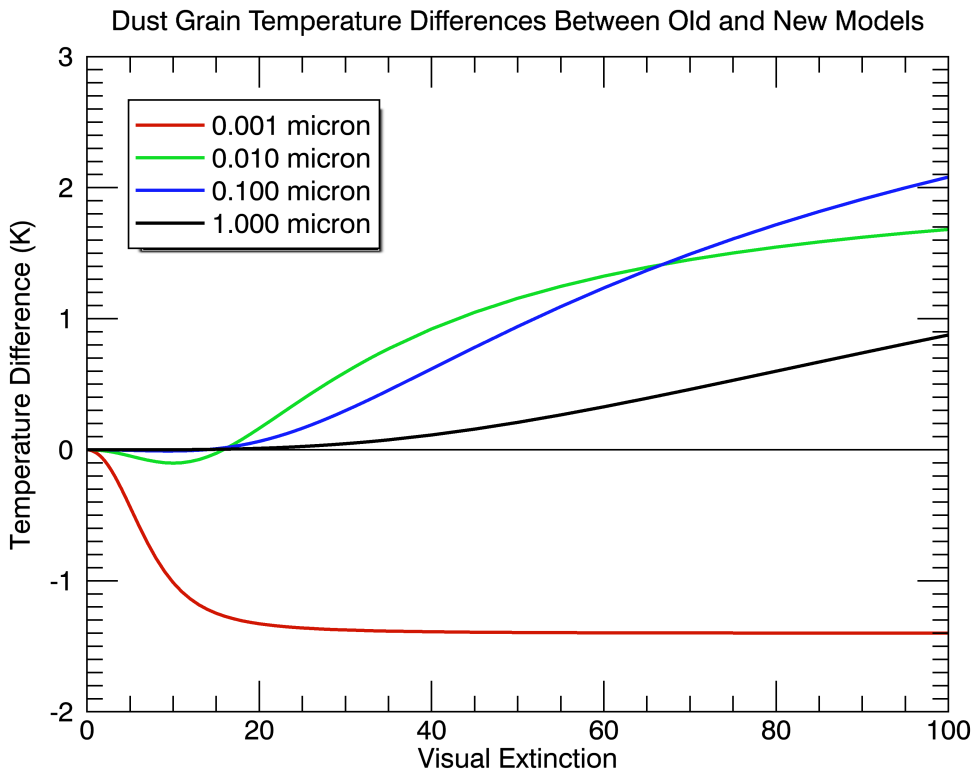

Figure 8 - This plot shows the dust temperature differences (new - old) between the models for different grain sizes at a gas temperature of 10 Kelvin

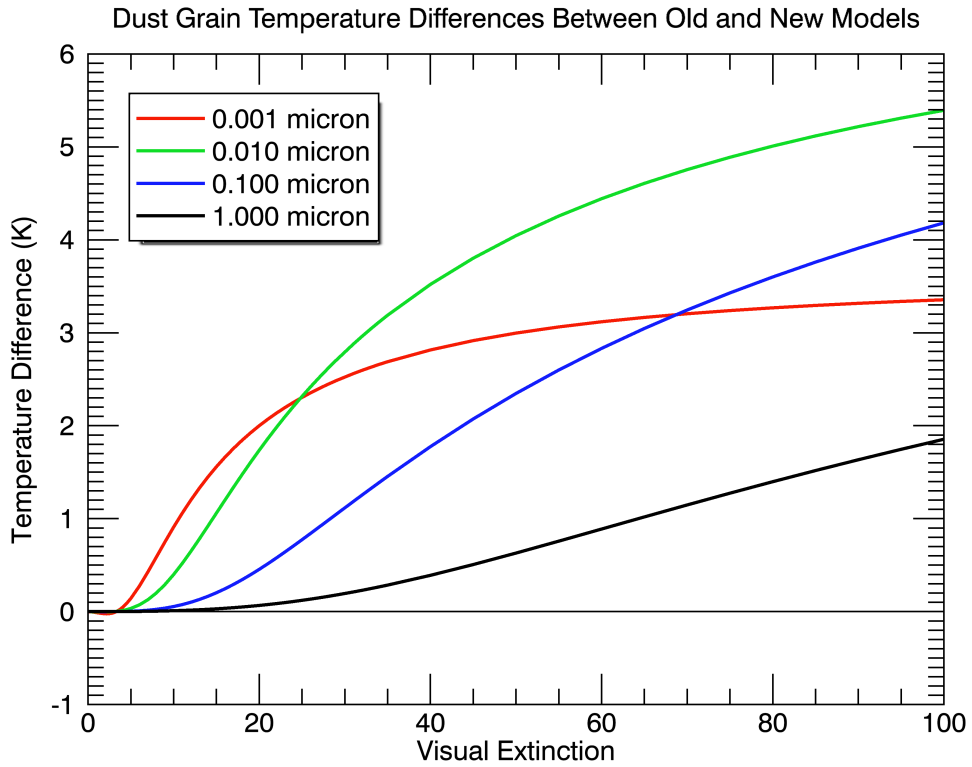

Figure 9 - This plot shows the dust temperature differences (new - old) between the models for different grain sizes at a gas temperature of 15 Kelvin

surface, as well as rates of absorption and desorption, which will in turn affect abundances in the gas phase and alter chemical processes that occur there.

Third, as previously stated, the results of this model have a strong dependence on grain size. This is very important for ISM models and may provide evidence for strong consideration of grain size as a significant parameter. For example, because the dust temperature can vary so largely over the range of possible grain sizes, under the same conditions, it may be worthwhile to consider using a more robust dust grain population in ISM models. Instead of using only one size, it may prove worthy to explore a dynamic profile of dust grain sizes and their relative densities in particular ISM cloud settings. There may be significant changes to the chemistry simulations to offset a potential increase in computational power needed. This is a potential avenue for further study in the future.

Acknowledgments

I would like to thank Professor Robin Garrod, my advisor, for directing me in this research endeavor and for helping me develop my skills over the course of the project. I would also like to thank the rest of the Garrod group for welcoming me onto their team and providing me support during my time with them. I hope this research can serve to compliment the good work they have been accomplishing, and will continue to do.

References

Draine, Bruce T. *Physics of the Interstellar and Intergalactic Medium*. N.p., 2011. *NASA ADS*. Web. 4 May 2017.

Garrod, Robin T. "A Three-Phase Chemical Model of Hot Cores: The Formation of Glycine." *The Astrophysical Journal* 765 (2013): 60. *NASA ADS*. Web.

Garrod, R. T., and T. Pauly. "On the Formation of CO2 and Other Interstellar Ices." *The Astrophysical Journal* 735 (2011): 15. *NASA ADS*. Web.

Garrod, Robin T., and Susanna L. Widicus Weaver. "Simulations of Hot-Core Chemistry." *Chemical Reviews* 113.12 (2013): 8939–8960. *ACS Publications*. Web.

Krügel, Endrik. *An Introduction to the Physics of Interstellar Dust*. N.p., 2008. *NASA ADS*. Web. 4 May 2017.

Zucconi, A., C. M. Walmsley, and D. Galli. "The Dust Temperature Distribution in Prestellar Cores." *Astronomy and Astrophysics* 376 (2001): 650–662. *NASA ADS*. Web.

Appendix

Look-up tables for dust temperature by visual extinction for a grain size of 0.1 micron and gas temperature of 10 Kelvin

Gas Density = 1.00E+04 cm^{-3}

Visual Extinction	Dust Temp (K)
0	19.9811
0.01	19.9535
0.0177828	19.932
0.0316228	19.894
0.0562341	19.8268
0.1	19.7087
0.177828	19.5028
0.316228	19.154
0.562341	18.5612
1	17.6156
1.2	17.2289
1.4	16.8756
1.6	16.5389
1.8	16.2211
2	15.9242
2.2	15.6441
2.4	15.3808
2.6	15.1329
2.8	14.8992
3	14.6788
3.2	14.4706
3.4	14.2748
3.6	14.0883
3.8	13.9114
4	13.7434
4.5	13.358
5	13.0152
6	12.4295
7	11.9463
8	11.5382
9	11.1872
10	10.8812
11	10.6115
12	10.3715
13	10.1562
14	9.96202
15	9.78587
16	9.62521
17	9.47816
18	9.34299
19	9.2183
20	9.10299
21	8.99593
22	8.89636
23	8.80341
24	8.71671
25	8.63525
26	8.55879
27	8.48683
28	8.41912
29	8.35515
31	8.23747
32	8.183
33	8.13128
34	8.08205
35	8.03533
40	7.83103
45	7.66546
50	7.52841
55	7.41336
60	7.31482
65	7.22979
70	7.15576
75	7.09073
80	7.03271
85	6.98119
90	6.93517
95	6.89365
100	6.85614

Gas Density = 1.00E+05 cm^{-3}

Visual Extinction	Dust Temp (K)
0	19.9668
0.01	19.9391
0.0177828	19.9176
0.0316228	19.8795
0.0562341	19.8122
0.1	19.6938
0.177828	19.4874
0.316228	19.1378
0.562341	18.5435
1	17.5951
1.2	17.2072
1.4	16.8527
1.6	16.5148
1.8	16.1958
2	15.8978
2.2	15.6166
2.4	15.3523
2.6	15.1034
2.8	14.8688
3	14.6475
3.2	14.4385
3.4	14.242
3.6	14.0548
3.8	13.8773
4	13.7087
4.5	13.3222
5	12.9786
6	12.3925
7	11.9103
8	11.5044
9	11.157
10	10.8555
11	10.5914
12	10.3579
13	10.1499
14	9.96364
15	9.79611
16	9.64457
17	9.50715
18	9.38184
19	9.26753
20	9.16271
21	9.06626
22	8.97756
23	8.89548
24	8.81965
25	8.74919
26	8.68372
27	8.62276
28	8.56579
29	8.51244
31	8.41587
32	8.37177
33	8.33042
34	8.29144
35	8.25446
40	8.09755
45	7.97559
50	7.87855
55	7.79952
60	7.73399
65	7.67897
70	7.6322
75	7.59218
80	7.55742
85	7.52691
90	7.5004
95	7.47664
100	7.45538

Gas Density = 1.00E+06 cm^{-3}

Visual Extinction	Dust Temp (K)
0	19.8231
0.01	19.7948
0.0177828	19.7729
0.0316228	19.734
0.0562341	19.6652
0.1	19.5441
0.177828	19.333
0.316228	18.9751
0.562341	18.3655
1	17.3897
1.2	16.9896
1.4	16.6234
1.6	16.274
1.8	15.9438
2	15.6352
2.2	15.3438
2.4	15.0698
2.6	14.812
2.8	14.5692
3	14.3403
3.2	14.1243
3.4	13.9217
3.6	13.729
3.8	13.5468
4	13.3742
4.5	12.9808
5	12.6347
6	12.0551
7	11.5931
8	11.2184
9	10.9105
10	10.6549
11	10.4409
12	10.2601
13	10.1064
14	9.97483
15	9.86145
16	9.76326
17	9.67768
18	9.60266
19	9.53663
20	9.47829
21	9.42632
22	9.37997
23	9.33849
24	9.30113
25	9.26734
26	9.23673
27	9.20893
28	9.18345
29	9.16021
31	9.11923
32	9.10112
33	9.08438
34	9.06889
35	9.05439
40	8.99543
45	8.9522
50	8.91934
55	8.89367
60	8.87312
65	8.85625
70	8.84232
75	8.83058
80	8.82052
85	8.8119
90	8.80453
95	8.79791
100	8.79216

Gas Density = 1.00E+07 cm^{-3}

Visual Extinction	Dust Temp (K)
0	18.3548
0.01	18.3208
0.0177828	18.2944
0.0316228	18.2476
0.0562341	18.1648
0.1	18.019
0.177828	17.7641
0.316228	17.3307
0.562341	16.591
1	15.4155
1.2	14.9427
1.4	14.5183
1.6	14.1232
1.8	13.7606
2	13.4328
2.2	13.1347
2.4	12.8653
2.6	12.6221
2.8	12.4028
3	12.2051
3.2	12.0267
3.4	11.8666
3.6	11.721
3.8	11.5892
4	11.4696
4.5	11.2159
5	11.0136
6	10.7163
7	10.5133
8	10.3685
9	10.2616
10	10.1804
11	10.1173
12	10.0673
13	10.0269
14	9.99377
15	9.96635
16	9.94334
17	9.92385
18	9.90721
19	9.89284
20	9.88038
21	9.86948
22	9.85991
23	9.85143
24	9.84388
25	9.83714
26	9.83109
27	9.82563
28	9.82069
29	9.8162
31	9.80836
32	9.80492
33	9.80175
34	9.79883
35	9.79613
40	9.7852
45	9.77731
50	9.77138
55	9.76678
60	9.76313
65	9.76015
70	9.7577
75	9.75563
80	9.75387
85	9.75237
90	9.75107
95	9.74993
100	9.74893